

# Calexcitin transformation of GABAergic synapses: From excitation filter to amplifier

MIAO-KUN SUN\*, THOMAS J. NELSON, HUI XU, AND DANIEL L. ALKON

Laboratory of Adaptive Systems, National Institute of Neurological Disorders and Stroke, National Institutes of Health, Bethesda, MD 20892

Communicated by Bernhard Witkop, National Institutes of Health, Bethesda, MD, April 8, 1999 (received for review February 2, 1999)

**ABSTRACT** Encoding an experience into a lasting memory is thought to involve an altered operation of relevant synapses and a variety of other subcellular processes, including changed activity of specific proteins. Here, we report direct evidence that co-applying (associating) membrane depolarization of rat hippocampal CA1 pyramidal cells with intracellular microinjections of calexcitin (CE), a memory-related signaling protein, induces a long-term transformation of inhibitory postsynaptic potentials from basket interneurons (BAS) into excitatory postsynaptic potentials. This synaptic transformation changes the function of the synaptic inputs from excitation filter to amplifier, is accompanied by a shift of the reversal potential of BAS–CA1 postsynaptic potentials, and is blocked by inhibiting carbonic anhydrase or antagonizing ryanodine receptors. Effects in the opposite direction are produced when anti-CE antibody is introduced into the cells, whereas heat-inactivated CE and antibodies are ineffective. These data suggest that CE is actively involved in shaping BAS–CA1 synaptic plasticity and controlling information processing through the hippocampal networks.

Synapses are considered a critical site at final targets through which memory-related events realize their functional expression (1), whether the events involve changed gene expression and protein translation, altered kinase activities, or modified signaling cascades. A few proteins have been implicated in associative memory. These include  $\text{Ca}^{2+}$ /calmodulin II kinases, protein kinase C (PKC), and calexcitin (CE), a recently cloned and sequenced 22-kDa learning-associated  $\text{Ca}^{2+}$ -binding protein (2, 3), and the type II ryanodine receptors (RyR). Levels of CE in identified mollusk neurons change with Pavlovian conditioning (3). CE is also a substrate of PKC and may play a role in pathophysiology of Alzheimer disease (2). It increases neuronal excitability in *Hermisenda* and mammalian hippocampus and cerebellum, whereas anti-CE antibodies react with 22-kDa protein fractions from mammalian brain extracts (2). Furthermore, biochemical and patch-clamp studies indicate that CE activates the RyR to release intracellular  $\text{Ca}^{2+}$  from the endoplasmic reticulum (2). These functional similarities in diverse species suggest homologous protein targets and mechanistic conservation across evolution.

## METHODS

**Chemicals.** Cloned CE (without the C-terminal P-loop) containing a His<sub>9</sub> leader sequence was expressed in BL21 (DE3) *Escherichia coli* cells and purified by repeated affinity chromatography on Ni<sup>2+</sup>-charged His-Bind columns (Novagen). Anti-CE antibody was raised in rabbits, by using peptide Ac-DVNDTSGDNIIDKHEYSTC-NH, corresponding to positions 115–133 of CE, conjugated to keyhole limpet hemocyanin (KLH; linked via C-terminal cysteine). The antibody was

effective against nondenatured CE only. Agents were either injected into the recorded cells through the recording electrodes: CE, anti-CE antibody, ruthenium red (RR), or 1,2-bis(2-aminophenoxy)ethane-*N,N,N',N'*-tetraacetic acid (BAPTA); or into the perfusion medium: kynurenic acid (KYN; Sigma; 500  $\mu\text{M}$ ; adjusted to pH 7.4 with 1 M NaOH; ref. 4), bicuculline methiodide (Sigma; 10  $\mu\text{M}$ ), acetazolamide (ACET; Sigma; 1 or 10  $\mu\text{M}$ ), or benzolamide (gift from T. H. Maren, University of Florida, Gainesville). For injections of the proteins, electrode tips were filled with 1  $\mu\text{l}$  (260 ng/ $\mu\text{l}$ ) of cloned CE, heat-inactivated CE, or anti-CE antibody or heat-inactivated anti-CE antibody, respectively, in 1 M potassium acetate (KOAc) and backfilled with 3 M KOAc (pH adjusted to 7.25). The proteins, BAPTA ( $\approx 10$  mM), and RR were injected during pulse cycles controlled with PCLAMP program (the proteins and BAPTA:  $-2.0$  nA, 700 ms on 33% duty cycles for 15 min; RR:  $+0.5$  nA, 500 ms 50% on duty cycles through 2 mM solution for 10 min). Heat-inactivated proteins (100°C for 5 min) were used as control. For carbonic anhydrase (CA) activity measurement, a 1- $\mu\text{l}$  sample of purified CA (Sigma) and rat brain homogenate in 1 ml of 0.1 M Tris-HCl (pH 7.4) was bubbled at 4°C with  $\text{CO}_2$  from a gas cylinder. pH changes were monitored with an Orion 9802 BH pH electrode connected to a data acquisition system via a VWR 8010 pH meter.

**Electrophysiology.** Male Sprague–Dawley rats (130–180 g) were decapitated and the brains were removed and cooled rapidly in a modified artificial cerebrospinal fluid (aCSF) ( $\approx 4^\circ\text{C}$ ), bubbled continuously with 95%  $\text{O}_2$ /5%  $\text{CO}_2$ . Hippocampi were sliced (400  $\mu\text{m}$ ), placed in oxygenated aCSF (124 mM NaCl/3 mM KCl/1.3 mM  $\text{MgSO}_4$ /2.4 mM  $\text{CaCl}_2$ /26 mM  $\text{NaHCO}_3$ /1.25 mM  $\text{NaH}_2\text{PO}_4$ /10 mM glucose), and subfused (2 ml/min) with the oxygenated aCSF in an interface chamber and allowed to equilibrate for a minimum of 1 hr at 30–31°C. Hepes was used to replace  $\text{NaHCO}_3$  in non-bicarbonate buffer solution, which was bubbled with 100%  $\text{O}_2$  (pH adjusted to 7.38–7.40). CA1 pyramidal cells were recorded intracellularly with sharp electrodes. Intracellular microelectrode recording rather than whole-cell clamp avoids immediate internal perfusion of the test proteins and agents into the cells and marked run-down of  $\gamma$ -aminobutyrate (GABA)-evoked currents. A control period without immediate influence of test proteins is crucial for evaluating test results. KOAc (3 M, pH 7.25)-filled electrodes (tip resistance 60–120 M $\Omega$ ) were positioned in the area of CA1. A bipolar stimulating electrode (Teflon-insulated PtIr wire 25  $\mu\text{m}$  in diameter) was also placed in the *stratum pyramidale*, within 200

Abbreviations: ACET, acetazolamide; BAPTA, 1,2-bis(2-aminophenoxy)ethane-*N,N,N',N'*-tetraacetic acid; BAS, basket neurons; CA, carbonic anhydrase; CE, calexcitin; EPSPs, excitatory postsynaptic potentials; GABA,  $\gamma$ -aminobutyrate; IPSPs, inhibitory postsynaptic potentials; KYN, kynurenate; PSP, postsynaptic potential; RR, ruthenium red; RyR, ryanodine receptors; SCH, Schaffer collateral pathway.

\*To whom reprint requests should be addressed at: Laboratory of Adaptive Systems/NINDS/NIH, Building 36, Room 4A24, 36 Convent Dr., Bethesda, MD 20892. e-mail: mksun@codon.nih.gov.

The publication costs of this article were defrayed in part by page charge payment. This article must therefore be hereby marked "advertisement" in accordance with 18 U.S.C. §1734 solely to indicate this fact.

PNAS is available online at www.pnas.org.

$\mu\text{m}$  from the recording electrode, for stimulation of basket interneurons (BAS) (50  $\mu\text{A}$ ). In some experiments, an additional bipolar electrode was placed in the *stratum radiatum* to stimulate the Schaffer collateral pathway (SCH). CA1 neurons with stable resting membrane potential more negative than  $-70$  mV were studied. Unless otherwise mentioned, test stimuli were applied at frequency of 1 per minute (0.017 Hz). Signals were amplified with AxoClamp-2B amplifier and digitized and stored by using a DigiData 1200 with the PCLAMP6 data collection and analysis software (Axon Instruments) and a Pentium PC computer. Experiments in which  $>20\%$  variations in the evoked inhibitory postsynaptic potentials (IPSPs) during a 10 min control period occurred were discarded. Percent baseline PSP at each minute was calculated by dividing its value by baseline PSP then multiplying the result by 100. Baseline PSP was the mean of 10 min before treatments in each cell. A negative sign was added to indicate its inhibitory nature so that  $-100\%$  is baseline IPSP and a positive value indicates an excitatory response. Differences were considered significant at  $P < 0.05$ .

## RESULTS

Effects of CE on synaptic function were investigated on synaptic inputs from GABAergic BAS to CA1 pyramidal cells. Each GABAergic interneuron powerfully inhibits some 1,000 pyramidal cells, providing widespread control over hippocampal networks (5–7). A single pulse stimulation within the *stratum pyramidale* produced IPSPs in CA1 pyramidal neurons at their resting membrane potential (Fig. 1*a*). The IPSPs ( $-8.4 \pm 0.3$  mV,  $n = 8$ ,  $P < 0.05$ ) were abolished (reduced by  $95.1 \pm 3.2\%$ ,  $n = 8$ ,  $P < 0.05$ , paired *t* test) by bicuculline (1  $\mu\text{M}$ , 30 min), a GABA<sub>A</sub> receptor antagonist (4), indicating that the evoked IPSPs are mediated largely, if not exclusively, by activation of BAS–CA1 pathway and are GABAergic. In some cases, a small but delayed inhibitory component remained in the presence of bicuculline (not shown), possibly representing an incomplete blockade of the GABA<sub>A</sub> receptor or GABA<sub>B</sub> receptor-mediated component.

KYN (4, 8), a competitive antagonist for both *N*-methyl-D-aspartate (NMDA) and non-NMDA ionotropic subtypes, receptors for the most dominant excitatory inputs to CA1 pyramidal cells, at 500  $\mu\text{M}$  (20 min; ref. 8) effectively eliminated SCH–CA1 excitatory postsynaptic potentials (EPSPs) (by  $>90\%$ ) but did not increase BAS–CA1 IPSPs (Fig. 1*b*). In the presence of KYN, the BAS–CA1 IPSP ( $-8.1 \pm 0.4$  mV,  $n = 7$ ,  $P < 0.05$ ) did not differ ( $P > 0.05$ ) from that of pre-KYN ( $-8.0 \pm 0.3$  mV,  $n = 7$ ,  $P < 0.05$ ), indicating the lack of a hidden, significant glutamatergic depolarizing component in the BAS–CA1 IPSPs.

The BAS–CA1 IPSPs were induced at different membrane potentials (Fig. 1*c* and *d*) and were found to reverse at a single membrane potential ( $-79.4 \pm 0.4$  mV,  $n = 59$ ). No minor

component was detected that exhibited a different reversal potential (Fig. 1*c* and *d*). The relationship between BAS–CA1 PSPs and membrane potentials can be described with a straight line, not affected by KYN (Fig. 1*e*). The reversal potential in the presence of KYN was  $-78.9$  mV ( $\pm 0.7$  mV) and did not significantly differ ( $n = 7$ ,  $P > 0.05$ ) from pre-KYN values ( $-78.7 \pm 0.6$  mV).

CE, applied postsynaptically into single pyramidal cells, produced a lasting ( $>1$  hr) reduction in BAS–CA1 IPSP (Fig. 1*f* and *j*; Table 1). The effect resulted from biological activity of CE, since heat-inactivated CE was ineffective (Fig. 1*g* and *j*; Table 1). Membrane input resistance was altered neither by CE (post-CE:  $83.7 \pm 2.5$  M $\Omega$  vs. pre-CE:  $83.6 \pm 2.6$  M $\Omega$ ,  $n = 10$ ,  $P > 0.05$ ) nor by heat-inactivated CE (post-CE:  $81.3 \pm 1.8$  M $\Omega$  vs. pre-CE:  $80.6 \pm 1.6$  M $\Omega$ ,  $n = 8$ ,  $P > 0.05$ ). Microinjections (with the same parameters used in the protocol) of CE conjugated with a green fluorescent Alexa488 resulted in strong labeling of the cell body and a portion of the dendritic tree in the plane of focus (Fig. 1*i* Left), indicating the efficacy of the CE microinjections. Similar intensity of labeling of the cells was observed when heat-inactivated conjugated CE was microinjected (Fig. 1*i* Right). Effects of CE on K<sup>+</sup> channels were evident as a reduction in after-hyperpolarization (from  $-4.7 \pm 0.3$  mV to  $-0.5 \pm 0.2$  mV,  $n = 10$ ,  $P < 0.05$ ) and a prolongation of the interval between brief intracellular depolarizing pulses (1 ms, 1–4 nA) sufficient to evoke action potentials and the time required for the membrane potential to repolarize to its prestimulation level (from  $39.5 \pm 1.9$  ms to  $53.4 \pm 2.3$  ms,  $n = 10$ ,  $P < 0.05$ ).

CE-induced reduction of BAS–CA1 PSPs does not appear to result from a simple blockade of a receptor–channel complex. Rather, CE caused a shift (Fig. 1*h*) of the relationship between BAS–CA1 PSPs and membrane potential to the right and of the reversal potential to more positive potentials (Table 1). The slope did not vary significantly on average. Heat-inactivated CE produced no such effect (Table 1).

When CE microinjection was coincident with postsynaptic depolarization (0.4–0.6 nA during the interval between injection episodes, to load Ca<sup>2+</sup>), the BAS–CA1 PSP was reversed to excitatory (Fig. 1*k* and *n* and Table 1). This synaptic transformation lasted more than 1 hr (Fig. 1*n*) and did not occur suddenly, but rather as an extension of an initial gradual reduction in BAS–CA1 IPSPs (Fig. 1*n*). The transformed synaptic response was eliminated by bath application of bicuculline (1  $\mu\text{M}$ ; 30 min; Fig. 1*o*; by  $95.6\% \pm 5.2\%$ ,  $n = 6$ ,  $P < 0.05$ ), indicating GABA<sub>A</sub> receptor mediation. The relationship between BAS–CA1 PSPs and membrane potential showed a further significant shift to the right with CE–depolarization pairing (Fig. 1*m*). Co-application of postsynaptic depolarization with heat-inactivated CE, however, had no such effects (Fig. 1*l* and *n*; Table 1).

Microinjections of anti-CE antibody, which recognizes CE-like proteins in rat and rabbit cerebellum and other brain

Table 1. Effects of CE on BAS–CA1 PSPs of CA1 pyramidal cells

Treatment	<i>n</i>	% PSPs			Reversal potential, mV		
		Control	Test	<i>P</i>	Control	Test	<i>P</i>
CE	10	$-101.1 \pm 4.2$	$-49.9 \pm 4.7^*$		$-79.0 \pm 1.0$	$-70.1 \pm 1.4^*$	
CE(I)	8	$-102.3 \pm 3.5$	$-106.0 \pm 3.6^{\text{NS}}$	$<0.05$	$-77.6 \pm 2.8$	$-78.0 \pm 2.4^{\text{NS}}$	$<0.05$
CE + Ca <sup>2+</sup>	10	$-102.3 \pm 2.4$	$+21.1 \pm 4.5^*$		$-77.5 \pm 0.9$	$-66.4 \pm 1.8^*$	
CE(I) + Ca <sup>2+</sup>	8	$-102.5 \pm 3.3$	$-99.2 \pm 2.5^{\text{NS}}$	$<0.05$	$-78.5 \pm 1.6$	$-78.8 \pm 1.7^{\text{NS}}$	$<0.05$
CE + Ca <sup>2+</sup> (BZA)	7	$-99.8 \pm 2.3$	$+23.4 \pm 3.7^*$	$>0.05^\dagger$	$-78.9 \pm 1.2$	$-67.2 \pm 2.0^*$	$>0.05^\dagger$
Anti-CE	8	$-100.4 \pm 3.1$	$-121.9 \pm 5.2^*$		$-79.5 \pm 0.9$	$-84.6 \pm 2.2^*$	
Anti-CE(I)	7	$-98.9 \pm 2.9$	$-100.9 \pm 3.1^{\text{NS}}$	$<0.05$	$-79.2 \pm 1.2$	$-79.6 \pm 1.8^{\text{NS}}$	$<0.05$

(I), heat-inactivated form; BZA, bath benzolamide. \*, Significant difference ( $P < 0.05$ ) as compared with pretreatments. NS, no significant difference ( $P > 0.05$ ) as compared with pretreatments. *P* indicates the significance of tests between the two groups;  $\dagger$ , as compared with CE + Ca<sup>2+</sup> group. Control values were obtained approximately 5 min before, while the test values were observed about 30 min after the application of the proteins.

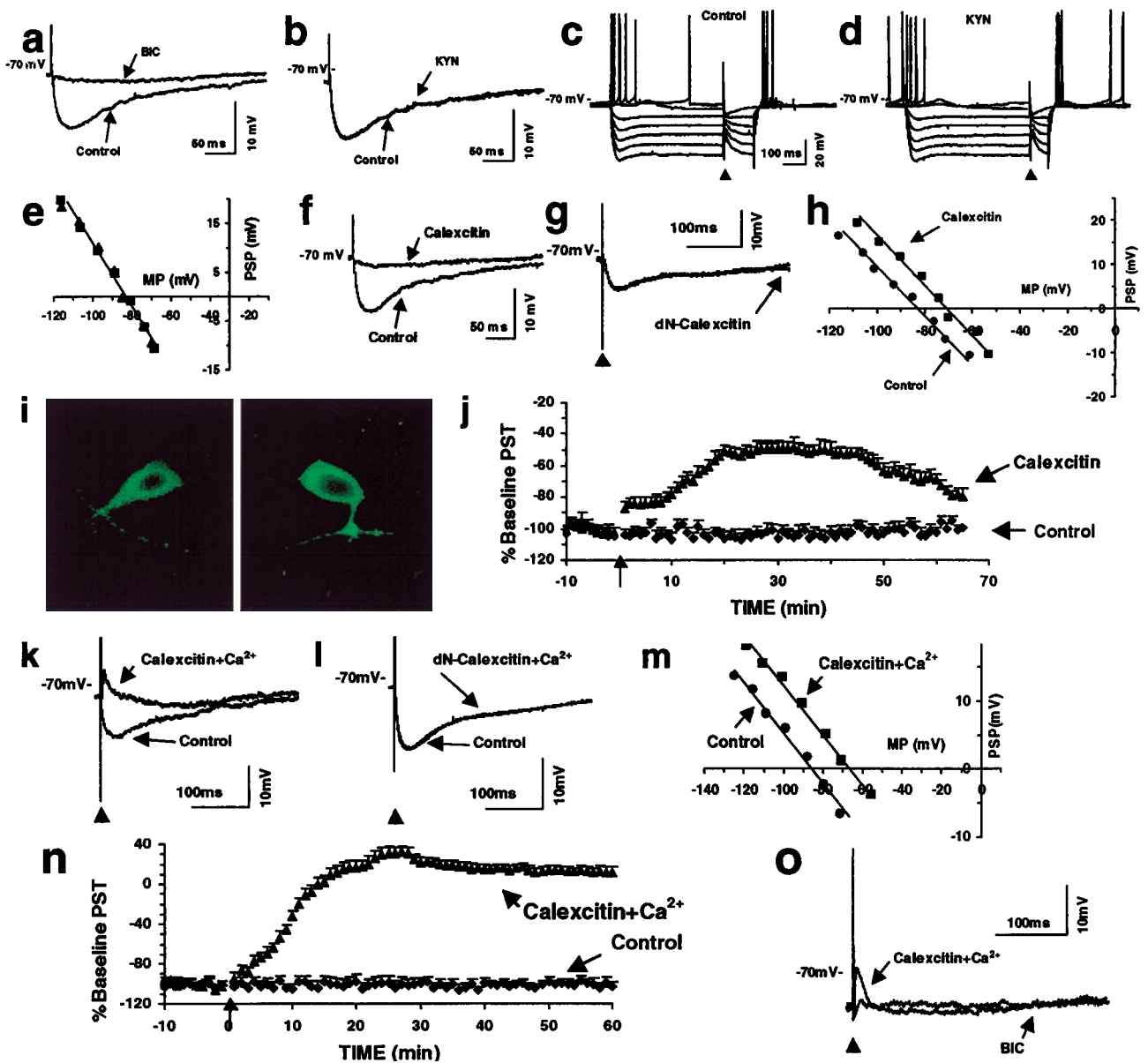


FIG. 1. CE transforms BAS-CA1 synapses. Bicuculline (BIC, 1  $\mu$ M, 30 min) eliminates (*a*), whereas KYN (500  $\mu$ M, 20 min) does not alter (*b*), the evoked IPSPs. The relationship between the evoked BAS-CA1 PSP at different membrane potentials (MPs) (*c* and *d*) in a CA1 pyramidal cell can be described with a straight line (*e*), determined by the least squares criterion, and is not altered by KYN (*c* and *d*). CE reduces BAS-CA1 IPSP (*f*; two overlapping traces) and shifts the PSP-MP curve to the right (*h*). Heat-inactivated CE (dN-Calyculin) is ineffective (*g*). Microinjections of CE conjugated with the green fluorescent Alexa488 (Molecular Probes) results in strong labeling of the cell body and portion of the dendrites in focus (*i*; *Left*, active form, and *Right*, heat-inactivated; after fixation with 10% paraformaldehyde/saline overnight and cutting to 40  $\mu$ m thick, shown  $\times 400$ ), indicating the efficacy of the CE microinjection. In *j*, time courses of the response to CE or heat-inactivated CE injection (Control), each point represents the mean IPSP magnitudes + SEM normalized to the average of the pre-CE IPSPs. PST, postsynaptic transformation. The vertical arrow indicates the time of injection. Associating CE injection with postsynaptic depolarization (0.4–0.6 nA during the off period with the current intensities adjusted to elicit 4–8 spikes per s) transforms BAS-CA1 inhibitory PSP into an excitatory one (*k*) and produces a further shift of the PSP-MP curve to the right (*m*). Associating heat-inactivated CE with postsynaptic depolarization (0.4–0.8 nA at the off period with current intensities adjusted to evoke 4–8 spikes per s) does not alter BAS-CA1 IPSP (*l*). Average responses of BAS-CA1 PSP after associating either CE (CE+Ca<sup>2+</sup>) or heat-inactivated CE (Control) are shown in *n*. The transformed synaptic response is eliminated by 1  $\mu$ M bicuculline (*o*; 30 min).

regions, including the hippocampus (T.J.N. and D.L.A., unpublished observations), into CA1 pyramidal cells produced a period of enhanced BAS-CA1 IPSPs (Fig. 2*a* and *d* and Table 1), whereas heat-inactivated anti-CE antibody was ineffective (Fig. 2*b* and *d* and Table 1). The difference, though small, was significant (Table 1). The anti-CE antibody-induced enhancement of BAS-CA1 IPSPs is not simply an increase in postsynaptic response for a given membrane potential. The relationship between BAS-CA1 IPSPs and membrane potential was shifted to the left (Fig. 2*c*). Thus, the antibody induced a significant change in the reversal potential to more negative

potentials (Table 1), whereas the heat-inactivated antibody was ineffective (Table 1). The membrane input resistance was not affected by microinjection of anti-CE antibody (post-antibody:  $79.0 \pm 3.2$  M $\Omega$  vs. pre-antibody:  $79.2 \pm 2.8$  M $\Omega$ ) or its heat-inactivated form (post-inactive antibody:  $80.7 \pm 4.1$  M $\Omega$  vs. pre-inactive antibody:  $80.6 \pm 3.0$  M $\Omega$ ). The IPSP enhancement by anti-CE antibody supports the idea that effects of CE on synaptic function are not an artificial change of synaptic function, but involve effects on endogenous substrates within the CA1 cells.

If reducing the GABA<sub>A</sub> receptor-channel Cl<sup>-</sup> current and increasing the HCO<sub>3</sub><sup>-</sup> current contributes to GABA-induced

depolarization (9, 10), the latter should be sensitive to CA inhibitors (9, 10).  $\text{HCO}_3^-$  formation is a slow process but is increased at least several thousandfold by CA (11), which is present within CA1 pyramidal cells (12). The  $\text{HCO}_3^-$  reversal potential is about  $-12$  mV (9) so that an outward flux would result (Fig. 2*e*) and thus depolarizes the membrane at resting membrane potentials. In the presence of ACET ( $1 \mu\text{M}$ , 30 min), a CA inhibitor, CE caused no obvious alterations in the BAS-CA1 IPSPs (Fig. 3*a*;  $-99.2 \pm 3.5\%$ , 30 min after CE injection as compared with  $-100\%$  control value,  $n = 8$ ,  $P > 0.05$ ). CA isoforms (such as cytoplasmic types I, II, III, and VII; cell-surface membrane type IV; mitochondrial type V; and secretory type VI; refs. 13 and 14) are zinc enzymes and show different sensitivity to ACET inhibition. Their activity can be regulated by hormones through cAMP in other tissues. Inhibition of probably the type II isoform ( $\text{IC}_{50} = 0.09 \mu\text{M}$  for ACET; ref. 13), in addition to a partial inhibition of other less sensitive isoforms, appears effective in suppressing the CE effect. Bath perfusion of the membrane-impermeant CA inhibitor benzolamide ( $10 \mu\text{M}$ ) was found to have no effects on the CE-induced synaptic transformation (Fig. 3*c* and Table 1), indicating that the inhibitory effects on CA were intracellular. At  $10 \mu\text{M}$  (30 min), ACET itself was sufficient to transform the BAS-CA1 IPSPs, while abolishing effects of CE on the synaptic response ( $n = 8$ , not shown). When non-bicarbonate buffer was perfused externally, a condition to minimize bicarbonate effects, CE did not elicit any obvious changes in BAS-CA1 IPSPs (Fig. 3*b*;  $-98.9 \pm 4.2\%$ , 30 min after CE injection as compared with  $-100\%$  control value,  $n = 7$ ,  $P > 0.05$ ). The cellular mechanism underlying the CE-induced GABAergic synaptic transformation thus involves an induction of a depolarizing  $\text{HCO}_3^-$  flux through the  $\text{GABA}_A$  receptor- $\text{Cl}^-$  channel (Fig. 2*e*; ref. 10). The effectiveness of CA

inhibitors and of minimizing bicarbonate influence indicates that altered  $\text{Cl}^-$  accumulation through changed activity of K-Cl transports is unlikely to be involved in the synaptic transformation. CE/ $\text{Ca}^{2+}$  may induce changes in anion selectivity of the  $\text{Cl}^-$  channels, activity of CA, and/or formation of  $\text{HCO}_3^-$  (Fig. 2*e*). Ion permeability of channels has been previously shown to be modifiable by intracellular messengers or cations/anions (15, 16).  $\text{Ca}^{2+}$ - and ATP-activated  $\text{HCO}_3^-/\text{Cl}^-$  conductance has been observed in nonneuronal cells (17). While these results strongly suggest a central role of  $\text{HCO}_3^-/\text{Cl}^-$  activity in the CE-induced synaptic transformation, CE, does not appear to directly affect CA activity, as determined by measuring pH changes in the reaction for  $\text{CO}_2$  conversion to bicarbonate in the presence of  $4.4$  nM CE,  $20 \mu\text{M}$   $\text{Ca}^{2+}$ , and  $6.6$  nM CA ( $384 \pm 18$  mmol/min·mg of CA,  $n = 4$ ; as compared with  $395 \pm 9$  mmol/min·mg of CA in the presence of  $4.4$  nM CE and  $20 \mu\text{M}$   $\text{Ca}^{2+}$ ,  $n = 6$ ;  $P > 0.05$ ). Nor was CA activity in the rat whole brain homogenate affected by  $4.4$  nM CE and  $10 \mu\text{M}$   $\text{Ca}^{2+}$  ( $1.32 \pm 0.07$  mmol/min·mg of protein,  $n = 2$ ; as compared with  $1.37 \pm 0.08$  mmol/min·mg of protein in the presence of  $4.4$  nM CE only,  $n = 2$ ;  $P > 0.05$ ). It thus remains to be determined what factors (coupled to CE and/or bound to  $\text{Ca}^{2+}$ ), which would be diluted to 1/10,000 in the brain homogenate, might affect CA and thereby mediate the responses. Retrograde inhibition of GABA release (18, 19), as induced by depolarizing the membrane potential to  $+60$  to  $+90$  mV, might not be involved in the CE-induced inhibition of the GABAergic IPSP that follows negative current pulses used to inject CE alone. Inhibition of GABA release would not be expected to produce a reversed membrane response in polarity, nor would it be expected to be sensitive to CA inhibition or non-bicarbonate buffering. The transformed response has also been observed in response to externally applied

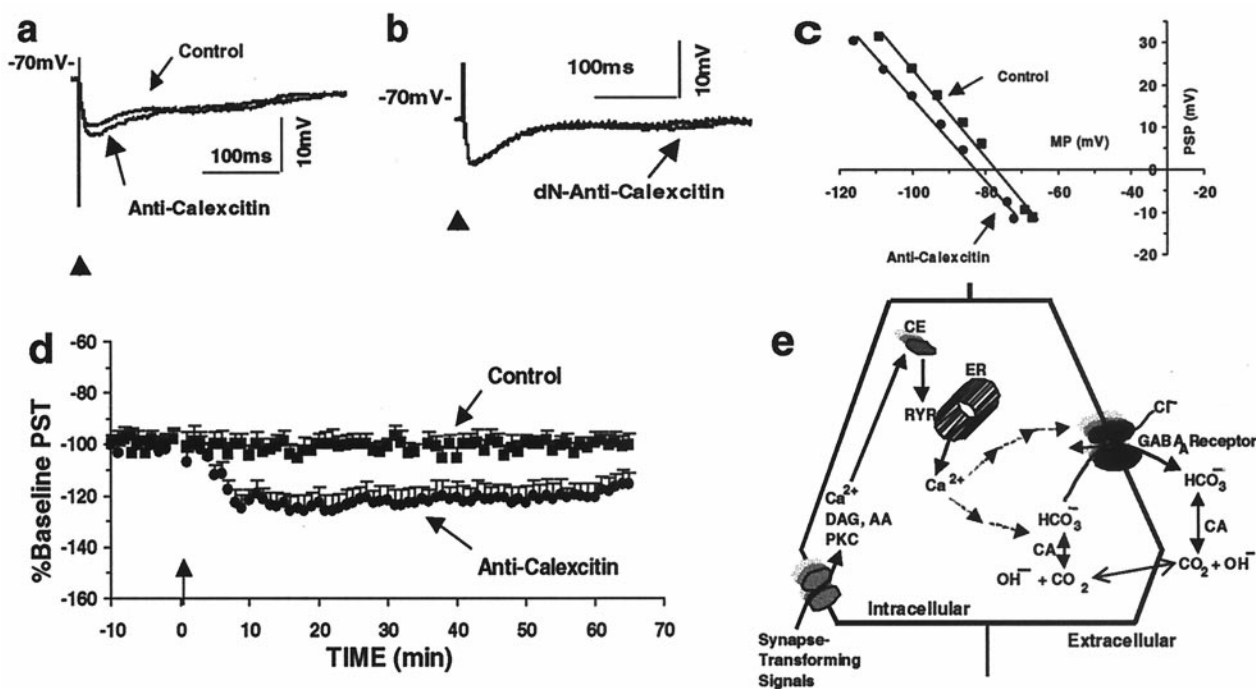


FIG. 2. Anti-CE antibody enhances BAS-CA1 IPSPs and mechanisms of CE-induced transformation of GABAergic synapses. Anti-CE antibody injection into a recorded CA1 pyramidal cell enhances BAS-CA1 IPSP (*a*, as compared with unmarked IPSP before injection) and elicits a shift of the PSP-MP curve to the left (*c*). Injection of heat-inactivated antibody is ineffective (*b*; two traces overlapping). Average responses of BAS-CA1 PSP after injection of either anti-CE antibody (Anti-CE) or its heat-inactivated form (Control) are shown in *d*. Schematic drawing (*e*) shows mechanisms of CE-mediated transformation of GABAergic synapses. Synapse-transforming signals (such as associative activation of cholinergic and GABAergic inputs) turn on a CE/CE-like protein signal cascade. CE binds to the RyR and causes  $\text{Ca}^{2+}$  release. The  $\text{Ca}^{2+}$ /CE transforms the GABAergic synapses by shifting the  $\text{GABA}_A$  reversal potential from  $\text{Cl}^-$  reversal potential toward  $\text{HCO}_3^-$  reversal potential, through altering anion selectivity of the  $\text{Cl}^-$  channels, activity of CA, and/or formation of  $\text{HCO}_3^-$ . Multiple arrows indicate possible involvement of unidentified mediators. AA, arachidonic acid; DAG, diacylglycerol; ER, endoplasmic reticulum; PKC, protein kinase C.

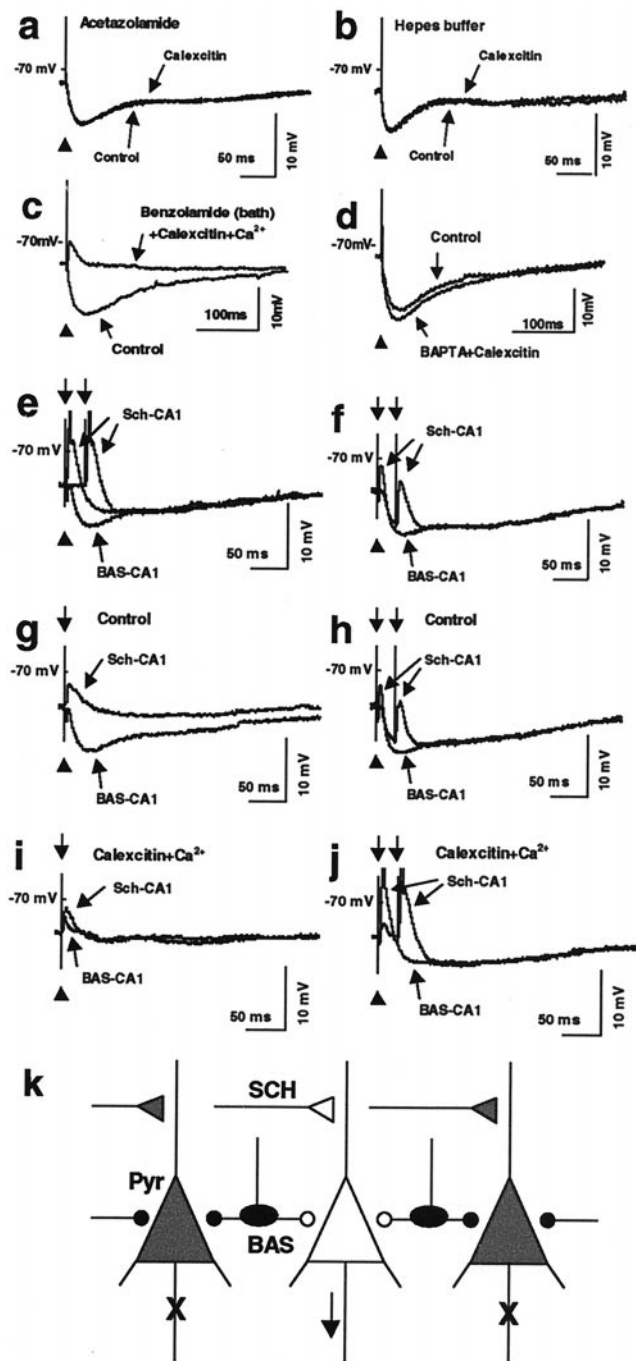


FIG. 3. ACET and non-bicarbonate buffer eliminate CE-induced transformation, and the transformation converts excitatory input filter into amplifier. ACET (1  $\mu$ M) eliminates CE-induced synaptic transformation (*a*). The effect of CE on BAS-CA1 IPSPs is not observed in HEPES buffer (*b*). In the presence of extracellular benzolamide (10  $\mu$ M), CE depolarization induces the synaptic transformation (*c*), which is not induced when BAPTA is co-applied (*d*); the charges carried by BAPTA are compensated by reducing the amount of acetate. Single-pulse stimulation (*e*) of BAS-CA1 evokes an IPSP and of SCH at above-threshold intensities, action potentials (truncated); two traces: one stimulated at delay of 10 ms and the other 30 ms, marked with arrows). The excitatory SCH (at the same above-threshold stimulation) input is filtered out by a costimulation of BAS-CA1 (*f*; two overlapping traces). (*g*) Single-pulse stimulation of BAS-CA1 evokes an IPSP, and stimulation of SCH at below-threshold intensities evokes an EPSP. The excitatory SCH (at the same below-threshold stimulation) input is below threshold as evoked by costimulation (single pulse) of BAS-CA1 and SCH inputs (*h*) before CE application. CE (30 min after the application) transforms BAS-CA1 IPSP and does not change

GABA (20) when paired with postsynaptic depolarization. Exogenous GABA (thus not under presynaptic control) delivered in the same quantity subsequently produced depolarization rather than hyperpolarization.

CE binds to the RyR in neurons and induces intracellular Ca<sup>2+</sup> release, as monitored with bis-fura-2 ratiometric imaging in rat CA1 pyramidal cells (2). We, therefore, examined whether the RyR may mediate effects of CE on BAS-CA1 synapses. RR, a membrane-impermeant polycationic molecule, inhibits the RyR with IC<sub>50</sub> in the nanomolar range and may alter its structure at micromolar concentrations. Its specificity is indicated by its lack of obvious effects on inositol trisphosphate receptor-mediated Ca<sup>2+</sup> release and ensured by postsynaptic application into singly recorded pyramidal cells (5 min before CE injection). RR slightly increased the evoked BAS-CA1 IPSPs (by 16.3%  $\pm$  4.0%,  $n = 10$ ,  $P < 0.05$ ), and it effectively blocked effects of CE on BAS-CA1 PSP ( $n = 10$ ). It neither reduced the GABAergic synaptic response nor affected postsynaptic membrane properties ( $n = 10$ ). Such changes would otherwise be expected if a significant amount of RR permeated (from inside the cell) the membrane to block voltage-sensitive Ca<sup>2+</sup> channels and presynaptic transmitter release during the experimental period. Buffering intracellular Ca<sup>2+</sup> with BAPTA mimicked RR in increasing the evoked BAS-CA1 IPSPs (by 17.4%  $\pm$  3.9%,  $n = 6$ ,  $P < 0.05$ ; Fig. 3*d*) and in blocking the effects of CE postsynaptic depolarization on the BAS-CA1 PSPs ( $n = 6$ ). These results, together with the previously obtained observations that CE induces intracellular Ca<sup>2+</sup> waves in hippocampal CA1 pyramidal neurons and release <sup>45</sup>Ca<sup>2+</sup> from microsomes (2), indicate that CE regulates intracellular Ca<sup>2+</sup> levels. The effectiveness of RR and BAPTA, however, does not rule out the possibility that Ca<sup>2+</sup> might function as a cofactor for CE and/or other mediators to induce changes in anion selectivity of the Cl<sup>-</sup> channels and activity of CA.

The BAS interneurons in CA1 are part of hippocampal networks that control the main excitatory input pathway and thus play a critical role in determination of information processing in CA1 pyramidal cells and memory storage, including transmission of the theta rhythm from septum to the hippocampus (21). In a separate study, we observed that GABAergic synaptic transformation can be induced through associative activation of the cholinergic-GABAergic inputs into the CA1 pyramidal cells (unpublished observations). Thus, CE-induced transformation of GABAergic synapses might help determine the synaptic effect of the cholinergic system during attention to training-induced stimulus association (22).

GABAergic interneurons receive excitatory inputs from SCH/commissural afferents in a feed-forward manner (6, 7, 23) and preferentially make synapses on cell bodies, proximal dendrites, and axon initial segments of CA1 pyramidal cells (7, 24). One BAS cell is estimated to have over 10,000 boutons innervating some 1,000 pyramidal cells (24), forming 10–12 synapses on each pyramidal cell (6, 7). The perisomatic termination of BAS cells is suited for synchronization of

much of the SCH-CA1 EPSP, evoked by single-pulse stimulation of BAS or SCH, respectively (*i*). The excitatory SCH (at the same below-threshold stimulation) input is amplified by the co-BAS stimulation after the CE-induced synaptic transformation and induces action potentials (truncated; *j*; two overlapping traces). (*k*) Schematic diagram of transformed GABAergic synapse functioning as either excitatory filter (surround) or amplifier (center). Active BAS GABAergic inputs effectively filter excitatory signals so that only very strong excitatory inputs might evoke action potentials. The GABAergic synaptic transformation results in amplifying excitatory signals so that weaker inputs can pass through the neural circuits (through the cell in the middle). BAS, basket GABAergic interneurons (in black); Pyr, CA1 pyramidal cells.

pyramidal cells (7). Modifiability of inhibitory circuits may thus be less specific but more efficient in controlling a specific population of pyramidal cells (7). Furthermore, the coincidence of GABAergic and the more specific glutamatergic inputs could confer great specificity in a center-surround manner (Fig. 3*k*). The transformed synaptic input from the BAS cells could provide a mechanism to selectively activate a subset of pyramidal neurons (those transformed and thus in the “center” of attention) and block others (those not transformed and thus in the “surround”). Activation of BAS produces fast IPSPs and reduces excitability (Fig. 3*e* and *f*) and probability of action-potential generation (25) of CA1 pyramidal cells. SCH stimulation at intensities above (30%) threshold elicits action potentials (100% of 10 trials; Fig. 3*e*). BAS stimulation produced an effective signal-filtering period of 50–100 ms (up to 200 ms in some cases), during which no action potential (0% of 10 trials) was evoked by SCH stimulation at the same intensities (Fig. 3*f*;  $n = 9$ ,  $P < 0.05$ ). Action potentials were reliably elicited (Fig. 3*j*;  $n = 9$ ) by single-pulse costimulation of SCH (at below threshold intensities) and BAS after CE-induced transformation (Fig. 3*i* as compare with Fig. 3*g*). Before the CE application, the same intensities of costimulation did not evoke action potentials (Fig. 3*h*;  $n = 9$ ). Weak signals are amplified in the transformed cells, whereas only very strong excitatory signals can successfully pass through the network under BAS inhibition. Thus, opposite GABAergic effects in subsets of neurons could act as either filter or amplifier, increasing the signal-to-noise ratio of relevant information, that is in the focused center of attention (Fig. 3*k*).

## DISCUSSION

Transformation of GABAergic inhibitory into excitatory synaptic potentials has been observed experimentally by several groups, with the transformed response lasting either for a short term (seconds to minutes; refs. 9 and 26–28) or a long period ( $\geq 1$  hr; refs. 20, 29, and 30). While fascinating and important, because the transformation results in a novel synaptic response, its role in memory and intracellular signaling cascades that lead to the synaptic transformation has remained obscure. The present study provides the evidence that lasting changes in synaptic polarity can be orchestrated by CE, an associative memory-related signal protein (2, 3). CE switches GABAergic synaptic function from excitation filter to amplifier and may help control hippocampal networks and hippocampus-dependent memory processing.

We thank Dr. T. H. Maren for kindly providing benzolamide.

1. Kornhauser, J. M. & Greenberg, M. E. (1997) *Neuron* **18**, 839–842.

2. Alkon, D. L., Nelson, T. J., Zhao, W. Q. & Cavallaro, S. (1998) *Trends Neurosci.* **21**, 529–537.
3. Nelson, T. J., Collin, C. & Alkon, D. L. (1990) *Science* **247**, 1479–1483.
4. Sun, M.-K. (1996) *Pharmacol. Rev.* **48**, 465–494.
5. McMahon, L. L. & Kauer, J. A. (1997) *Neuron* **18**, 295–305.
6. Buhl, E. H., Halasy, K. & Somogyi, P. (1994) *Nature (London)* **368**, 823–828.
7. Cobb, S. R., Buhl, E. H., Halasy, K., Paulsen, O. & Somogyi, P. (1995) *Nature (London)* **378**, 75–78.
8. Collingridge, G. L. & Lester, A. J. (1989) *Pharmacol. Rev.* **40**, 143–209.
9. Staley, K. J., Soldo, B. L. & Proctor, W. R. (1995) *Science* **269**, 977–981.
10. Grover, L. M., Lambert, N. A., Schwartzkroin, P. A. & Teyler, T. J. (1993) *J. Neurophysiol.* **69**, 1541–1555.
11. Dodgson, S. J., Tashian, R. E., Gros, G. & Carter, N. D. (1991) *The Carbonic Anhydrases* (Plenum, New York).
12. Paternack, M., Voipio, J. & Kaila, K. (1993) *Acta Physiol. Scand.* **148**, 229–231.
13. Landolfi, C., Marchetti, M., Ciocci, G. & Milanese, C. (1997) *J. Pharmacol. Toxicol. Methods* **38**, 169–172.
14. Linskog, S. (1997) *Pharmacol. Ther.* **74**, 1–20.
15. Williams, K., Pahk, A. J., Kashiwagi, K., Masuko, T., Nguyen, N. D. & Igarashi, K. (1998) *Mol. Pharmacol.* **53**, 933–941.
16. Rychkov, G. Y., Pusch, M., Roberts, M. L., Jentsch, T. J. & Bretag, A. H. (1998) *J. Gen. Physiol.* **111**, 653–665.
17. Ishikawa, T. (1996) *J. Membr. Biol.* **153**, 147–159.
18. Alger, B. E., Pitler, T. A., Wagner, J. J., Martin, L. A., Morishita, W., Kinov, S. A. & Lenz, R. A. (1996) *J. Physiol. (London)* **496**, 197–209.
19. Marty, A. & Llano, I. (1995) *Curr. Opin. Neurobiol.* **5**, 335–341.
20. Collin, C., Devane, W. A., Dahl, D., Lee, C.-J., Axelrod, J. & Alkon, D. L. (1995) *Proc. Natl. Acad. Sci. USA* **92**, 10167–10171.
21. Toth, K., Freund, T. F. & Miles, R. (1997) *J. Physiol. (London)* **500**, 463–474.
22. Fisahn, A., Pike, F. G., Buhl, E. H. & Paulsen, O. (1998) *Nature (London)* **394**, 186–189.
23. Paulsen, O. & Moser, E. I. (1998) *Trends Neurosci.* **21**, 273–278.
24. Halasy, K., Buhl, E. H., Lorinczi, Z., Tamas, G. & Somogyi, P. (1996) *Hippocampus* **6**, 306–329.
25. Andreasen, M. & Lambert, J. D. (1998) *J. Physiol. (London)* **507**, 441–462.
26. Wong, R. K. S. & Watkins, D. J. (1982) *J. Neurophysiol.* **48**, 938–951.
27. Kalia, K., Lamsa, K., Smirnov, S., Taira, T. & Voipio, J. (1997) *J. Neurosci.* **17**, 7662–7672.
28. Taira, T., Lamsa, K. & Kaila, K. (1997) *J. Neurophysiol.* **77**, 2213–2218.
29. Alkon, D. L., Sanchez-Andres, J.-V., Ito, E., Oka, K., Yoshioka, T. & Collin, C. (1992) *Proc. Natl. Acad. Sci. USA* **89**, 11862–11866.
30. Alkon, D. L., Lederhendler, I. & Soukimas, J. J. (1992) *Science* **215**, 693–695.